11th International Workshop on Inelastic Ion Surface Collisions
Wangerooge, Germany, September 22-27, 1996

On the Neutralization of Singly and Multicharged Projectiles During Grazing Interactions with LiF(100)

F. W. Meyer[1], Q. Yan[1], P. Zeijlmans van Emmichoven[2], I.G. Hughes[3], and G. Spierings[2]

[1]*Oak Ridge National Laboratory, Oak Ridge, Tennessee 37831-6372*

[2]*Debye Institute, Utrecht University, Princetonplein 5, 3584 CC Utrecht, The Netherlands*

[3]*Department of Pure and Applied Physics, The Queens University of Belfast, Belfast, United Kingdom*

Abstract

Measurements are reported of scattered neutral fractions for Na, K, Cs, and Ne singly and multicharged ions, and of scattered negative ion fractions for incident O, F, and B projectiles grazingly incident on LiF(100) as function of projectile velocity. In the case of the Na and Ne incident ions, significant dependence of the scattered neutral fractions on incident charge state is found, which is most pronounced at the lowest investigated velocities. Possible reasons for the observed initial charge state dependence are considered. In addition, results are reported for the target azimuthal dependence of the final neutral fraction observed for grazingly incident 35 keV Cs^{+7} ions.

keywords: electron transfer, alkali halides, image acceleraction, multicharged ion

INTRODUCTION

Studies of the interaction of singly and multicharged ions with solid targets have recently been expanded to include alkali halide surfaces [1–5]. So far, the understanding of the physics underlying the interactions with insulator targets is still increasing, but not yet comparable to that achieved for metal targets [6]. For example, in the area of negative ion formation, the target states involved are still the subject of active discussion. Measurements by R. Souda et al. [7] suggest that negative ion formation occurs preferentially during interactions with states localized at the alkali lattice sites, while results of Auth et al. [4] have been interpreted in terms of binary interactions with the halogen sites. In addition, some complimentary insulator studies have arrived at seemingly contradictory conclusions, adding to the puzzle. For example, measurements by Auth et al. [3] of image charge acceleration of multicharged Xe ions in front of a LiF surface suggested significant projectile neutralization (i.e. "hollow atom" production) prior to impact on the LiF surface. First measurements of KLL Auger spectra for N^{6+} incident on LiF(100) reported by Limburg et al. [2], on the other hand, indicated an absence of features associated with above surface KLL emission, casting doubt on the existence of "hollow atoms" above such surfaces.

For metal targets, the position of the Fermi level with respect to the relevant empty atomic level of the interacting projectile determines the open (i.e. energetically allowed) neutralization channels, which in turn manifest themselves in the characteristic velocity dependences observed in scattered neutral and negative ion fractions resulting from grazing interactions of incident positive ions. For such targets it has been observed for a number of cases for incident charge states 2+ or greater, that the measured scattered neutral fractions depend, if at all, only relatively weakly on incident projectile charge [8], indicating that charge equilibration had been essentially reached prior to the final phase of the projectile neutralization that occurs on the receeding trajectory, and suggesting, by what appears to be an only slight generalization, that charge fraction measurements using incident multicharged ions give results that mirror those for singly charged ions incident at the same velocity.

In the present article, we explore the validity of this assumption in the case of a LiF target

DISCLAIMER

for various incident positive ions, by presenting measurements of scattered neutral fractions for singly and multicharged Na, and Ne ions, and for multicharged K, and Cs ions, and of scattered negative ion fractions for singly and multicharged O, F, and B projectiles incident on LiF(100). For the case of the incident Na and Ne ions, the scattered neutral fractions for multicharged incident ions are found to be significantly **higher** than those for incident singly charged ions, particularly at the lowest investigated velocities. On the other hand, the scattered negative ion fractions for incident O and F ions were found to be virtually independent of projectile charge. In an attempt to probe the local vs. non-local nature of the neutralization process in the case of a LiF target, we also present first measurement results for the target azimuthal dependence of the scattered neutral fraction for incident 35 keV Cs^{7+} ions.

EXPERIMENTAL APPROACH

With exception of the added C foil in front of the detector, the apparatus used for the present measurements has been previously described [8,16,10]. The target sample was cleaved from a LiF single crystal in air and quickly put into a UHV chamber having a base pressure of 3×10^{10} mbar. Surface preparation consisted of 30 min. annealing cycles at a temperature of roughly 400°C. The sample temperature was kept at about 300°C during the measurement in order to avoid target charging. The surface quality was checked by verifying the presence of characteristic banana shaped channeling patterns for ions grazingly incident along low index channeling directions. The charge state distribution of the scattered (reflected) projectiles was measured by selecting a thin vertical slice of the scattered beam with movable slits, which was then dispersed by charge state across the face of a 40 mm diameter two dimensional position sensitive detector (PSD) using a pair of electrostatic deflection plates. A centered 3.5 $\mu g/cm^2$ 12 x 40 mm C foil mounted on a 90% transmission Ni mesh located roughly 5 mm upstream of the first MCP was added for the present measurements, and could be used to investigate charge or quantum state dependent detector efficiency effects [11] on the measured charge fractions. This was accomplished by comparing composite charge fraction spectra aquired in the foil region for different vertical PSD positions with similar composite spectra acquired in those PSD regions not covered by the C foil. For the case of Ne and Na projectiles, foil transmission was sufficient to permit such determinations down to energies of about 7 keV. The zero degree position on the PSD and the angle of incidence on the LiF sample were accurately determined by monitoring with the PSD a photon beam produced by illuminating the ion collimation section upstream of the sample with a UV light source, and registering its shift after specular reflection from the LiF sample. Beam intensities on target were kept sufficiently low to avoid significant defect formation as well as to avoid count rate saturation of the PSD.

RESULTS AND DISCUSSION

Figure 1 shows measured scattered neutral fractions for multicharged Cs, K, and Na ions (q=2-7) grazingly incident on LiF(100) as function of projectile velocity. It is noted that for this range of measured charge states, the measured neutral fractions were largely independent of initial projectile charge. As can be seen from the figure, the scattered neutral fraction for the Na projectiles exceeds ~60% at the lowest investigated velocities and, for the K projectiles as well, decreases with increasing velocity over the whole velocity range investigated. For the Cs projectiles, on the other hand, the neutral fraction goes through a local maximum of ~18% at a velocity of 0.16 a.u.

Under the assumption that the above results are representative of singly charged incident ions as well, the velocity dependence of the scattered alkali neutral fractions would be strongly suggestive of the involvement of a resonant electron transfer process in the formation of the dominant scattered charge fraction during the final phase of the ion surface interaction. Since electronic transitions between the LiF valence band and the alkali neutral atomic levels would be clearly non-resonant (by at least 7 eV), a hypothesis that the resonant transitions involve occupied surface states [12] located in the upper half of the LiF band gap has been made, and a simple theory developed [12] which reproduces the experimental data surprisingly well. In view of the results presented below, however, this scenario must be considered with increased caution. Shown in Figs. 2 and 3 are comparisons of angular distributions in scattered charge fractions for 5 keV Na singly, and doubly or triply charged projectiles incident on LiF at two different geometric grazing angles. As can be seen from Figure 2, at the smaller incidence angle, there is almost an order of magnitude difference between the observed neutral fractions, with the neutral fraction for incident Na^{+2} exceeding 40%, and that for incident Na^{+} amounting to approximately 5%, in good agreement with unpublished results of H. Winter [13]. At the larger incidence angle shown in Figure 3, the difference is reduced to a factor of roughly 3-4, primarily due to the significant perpendicular velocity dependence manifested by the 1+ incident neutral fraction. This perpendicular velocity dependence is opposite to that observed for higher incident charge states, as illustrated in Figure 4 for the case of incident Cs multicharged ions. Preliminary measurements of the scattered charge fractions for 7 keV incident Na ions with and without foil, indicate that, at least at this energy, charge or quantum state dependent detector efficiency effects are at the 20-30% level, slightly favoring detection of neutrals. It is noted in passing that the total scattering angles of the neutrals for the two different charge states shown in Figures 2 and 3 are different, despite identical target settings, due to the different image acceleration energy gains experienced by the different incident charge states. A more detailed analysis of these differences is deferred to a later publication [14], where formation distances will be deduced from the energy gains of the different charge states. Slight differences in total scattering angles as well as the widths of the respective distributions for the neutral and singly charged fractions evident for the two different incident charge states will also be analyzed in greater detail at that time in an attempt to gain more insight into the physical basis underlying the large observed scattered neutral fractions for the incident multicharged ions.

One characteristic of the multicharged alkali projectiles that might be responsible for the observed charge dependence is the fact that, unlike the singly charged ones, which have no electron capture levels that are even remotely resonant with the LiF valence band, the higher charged projectiles have numerous such levels (albeit excited). This difference in available resonant capture states for incident Na^+ and Na^{+2} ions is shown in Figure 5. On the other extreme of neutral binding energies, there are the noble gas projectiles, whose neutral binding energies fall well below the bottom of the LiF valence band, but which have numerous excited levels in the higher charge states that are (quasi)resonant with the LiF valence band. The energy level structure of Ne is included in Figure 5 as a good example of this case, since, in the absence of broadening effects, the alternate Auger neutralization mechanism is also energetically blocked in the case of the incident singly charged ion. As with the incident Na projectiles, significant differences were observed in scattered neutral fractions measured for incident singly charged and multicharged Ne projectiles.

Figure 6 shows our results for this system, as well as those of Hecht et al. [15] for incident Ne^+ ions. At velocities roughly exceeding 0.15 a.u., the measured scattered neutral fractions are truly initial charge state independent, giving the same large fractions for incident 6+ as well as 1+ ions. Below this energy, however, a systematic lowering of the neutral fractions is observed with decreasing incident charge state, amounting to a 25% reduction at v=0.1 a.u. (going from 6+ to 1+), with the diffferences becoming even greater with the lower velocities. In amanner similar to that discussed for the Na projectiles, we have made detailed comparisons in the scattered neutral and 1+ charge fractions and their angular distributions at 4.5 keV for incident 1+ and 3+ Ne projectiles for two different grazing incident angles. The results are shown in Figures 7 and 8. As can be seen, at both incidence angles, the difference in neutral fractions has reached a factor of about 2 at this energy, but, unlike the Na case, does not show significant dependence on perpendicular velocity. More interesting, at both incidence angles, there is now a clear difference in the scattered neutral-singly charged angular distribution offsets between incident 1+ and 3+ projectiles, suggesting a difference in final formation distances on the receding trajectory of the scattered 1+ ions for the two different projectiles. It is noted that, as with the Na projectiles, charge and quantum state dependent detection efficiency effects were investigated in a preliminary fashion at 7 keV, and found to be below the 20% level at that energy, with detection of neutrals again slightly favored, the effect decreasing with increasing energy.

For completeness we show in Figure 9 measurements similar to those shown in Figure 6, but for a NaF(100) target. Again differences in the scattered neutral charge fractions are observed as function of incident charge state, only smaller in magnitude. It is speculated that the smaller observed effect is due to the fact that the top of the NaF valence band is sufficiently closer to the vacuum level so that, unlike for the LiF target, Auger neutralization becomes a more efficient alternate neutralization pathway for the incident singly charged Ne ion.

For both investigated species, the observed charge state dependence thus appears to be due to a blocking of the neutralization for the singly charged ion, and which can be bypassed in some manner by projectiles in higher charge states. At least two possibilities by which the bypass may occur involve population of excited states. The first is quasi-resonant double electron capture by a doubly charged incident Ne or Na projectile to form a doubly excited neutral. For both species Hartree Fock calculations [16] reveal doubly excited levels lying within one or two eV of the top of the LiF valence band. The second is sequential single electron capture, the first electron being captured to form an excited 1+ core, the second to a level more tightly bound (due to reduced screening) than the corresponding level bound to a ground state 1+ core, consequently lying closer in energy to the valence band. The key point with either pathway is the manner in which the doubly excited state relaxes. For metal targets this relaxation is a competition between resonance ionization (with probably the fastest rate), in the event the doubly excited state lies energetically in the conduction band, auto-ionization, and Auger de-excitation. Due to the fordidden band gap in the alkali halide target, the first channel is effectively blocked, with possible exception of very loosely bound levels that are resonant with higher lying empty surface states [18,17]. Autoionization would fill the core hole, but eject the outer captured electron, and thus not avoid the blocked neutralization of the 1+ ion. Auger de-excitation, on the other hand, as illustrated in Figure 10 for the incident Na^{2+} ion, leaves the projectile charge unchanged (ejecting instead a valence band electron) and thus effectively bypasses the neutralization "bottleneck" presented to the 1+ projectile. Obviously, more detailed modeling of this scenario is called for, based on realistic rates for the two competing relaxation processes. It does seem clear, however, that the bypass is facilitated in the case of the insulator targets, for which the resonance ionization pathway is eliminated. This is illustrated in Figure 11, which shows previously published [8] results for the scattered neutral fraction of Na^{q+} ions grazingly scattered from Au(110). For the gold target, the measurements reveal the kinematic resonance [19–21] velocity dependence characteristic of the Na^{+} incident ion, even though they were carried out with incident charge states 2-9. It is speculated that for the Au(110) target, efficient resonance ionization of the doubly excited states into the metal conduction band closes the pathway that could have effectively bypassed the slow neutralization of 1+, thereby eliminating the incident charge dependence effect so prominent for the Na projectiles interacting with LiF.

We now turn to systems for which the scattered charge fractions measured for incident charge states greater than 1+ appears to correspond with only minor deviations to those observed for incident 1+ ions. We show first in Figure 12 our results for the observed scattered negative ion fractions for grazingly incident O, and F ions in the projectile velocity range 0.12 - 0.56 a.u. Fractions for both projectile species show characteristic kinematic resonance peak shapes, with maxima for incident F and O projectiles approaching 80% and 60%, respectively, in good agreement with the results of Auth et al. [4] for incident singly charged ions. Also shown are results for incident multicharged B projectiles for which maximum negative ion yields approaching 3% are observed, but for which the corresponding measurements for singly charged incident ions have not yet been carried out.

Figure 13 shows results for the scattered neutral fractions resulting from grazing interactions of Ar multi and singly charged ions with LiF. The present results are in reasonable agreement with the measurements of Hecht et al. [15] for singly charged incident projectiles at the lowest investigated velocities, but seem to drop more steeply with increasing velocity, possibly due to charge state dependent detection efficiency effects which have not yet been investigated for the incident Ar charge states, or possibly due to differences in incidence angles employed in the two measurements. It is noted that for incident O, F, and Ar ions, the ground state neutral levels are all either resonant or very close in energy to the bottom of the LiF valence band, and that incident singly charged ions of the latter species are thus well positioned energetically for efficient resonant neutralization from the LiF valence band.

We conclude by presenting initial results of measurements aimed at elucidating the local or non-local nature of the interaction responsible for projectile neutralization during collisions with LiF. To that end we have investigated the target azimuth dependence of the scattered neutral fraction observed for grazing impact of 35 keV Cs^{+7} ions. The measurement results are presented in Figure 14. As can been seen from the figure, a sharp drop in the measured scattered neutral fraction is observed for projectiles traveling along the <100> direction of the (100) surface. Along this direction, each lattice row consists of alternating Li and F sites. It is tempting to conclude from the observed azimuth dependence that the projectile neutralization takes place preferentially, in line with the findings of Souda et al. [7], at the Li sites, which are obscured in the <100> direction particularly at grazing incidence angles, due to the significantly larger radii of the F sites. However, additional measurements are needed, e.g. for the corresponding situation with incident singly charged Cs ions. It is noted that, in contrast to the Cs results, similar measurements [14] made of the azimuthal dependence of the scattered negative fraction for incident O projectiles show a pronounced and narrow enhancement around the <110> direction, along which the Li sites are fully exposed, and an only weak and relatively broad drop around the <100> direction. Furthermore, all the above azimuthal features are prominent only at low parallel velocities, and were not observable at much higher energies. Clearly more work is needed in this area before more definitive conclusions can be reached.

CONCLUSIONS

In summary, the velocity dependences of neutral and negative charge fractions have been measured for a variety of singly and multicharged ions incident on LiF. For incident Ne, and Na projectiles, a significant **enhancement** was observed in scattered neutral fractions when multicharged ions were used over those observed for singly singly charged incident ions, particularly at the lowest investigated velocities. This effect was interpreted as arising from the blocking of neutralization of singly charged projectiles due to lack of available levels quasi-resonant with the target valence band, and the bypassing of this bottleneck by more highly charged projectiles via capture into excited states which can relax by Auger de-excitation. This situation is in contrast to that found for metal targets, where resonance ionization to the target conduction band appears to effectively terminate this pathway. For insulator targets therefore, great care needs to be exercised when attempting to deduce the nature of interactions operative for singly charged incident projectiles from corresponding observations made with multicharged projectiles.

ACKNOWLEDGEMENTS

We would like to thank D. M. Zehner and N. Tolk for providing the alkali halide samples, and to acknowledge stimulating discussions with J. Burgdörfer and C. Reinhold. We further thank H. Winter for helpful comments and for communication of results prior to their publication. Q. Yan was supported through a program administered by the Oak Ridged Institute for Science and Education. This research was sponsored by the Office of Fusion Energy Sciences, and by the Office of Basic Energy Sciences of the U.S. Department of Energy under contract No. DE-AC05-96OR22464 with Lockheed Martin Energy Research Corp.

REFERENCES

[1] M. Vana et al., Europhys. Lett. **29**, 5560 (1995); Nucl. Instrum. Methods. B**100**, 284(1995).

[2] J. Limburg, et al., Phys. Rev. Lett. **75**, 217 (1995).

[3] C. Auth, et al., Phys. Rev. Lett. **74**, 5244 (1995).

[4] C. Auth, et al., Phys. Rev. Lett. **75**, 2292 (1995).

[5] H. Winter, C. Auth, and A.G. Borisov, NIM B (1996).

[6] J. Burgdörfer et al., Phys. Rev. A **44**, 5647 (1991).

[7] R. Souda et al., Surf. Sci. **324** L349 (1995).

[8] Q. Yan, S. Schippers, D.M. Zehner, and F.W. Meyer, Phys. Rev. A **54**, 641 (1996).

[9] L. Folkerts et al., Phys. Rev. Lett. **72**, 2204 (1995).

[10] F. W. Meyer et al., Nucl. Instrum. and Methods B**100**, 366 (1995).

[11] H. Winter, Nucl. Instrum. and Methods B**78**, 38 (1993).

[12] Q.Yan and F.W. Meyer, contributed paper to ICDIM 96, Wake Forest Univ. 15-19 July, 1996, to be published by Trans Tech Publ. Ltd. (Switzerland).

[13] H. Winter, private communication (1996).

[14] Q. Yan, et al., to be submitted to Phys. Rev. A.

[15] T. Hecht, C. Auth, A.G. Borisov, and H. Winter, submitted to Phys. Rev. Lett. (1996).

[16] R.D. Cowan, *The Theory of Atomic Structure and Spectra*, (University of California Press, Berkeley, 1981).

[17] P. Wurz and C. H. Becker, Surf. Sci. **224**, 559 (1989).

[18] G. Roy, et al., Surf. Sci. **152/153**, 1042 (1985).

[19] H. Schröder and E. Kupfer, Z. Physik F **279**, 13 (1976); J. Burgdörfer and E. Kupfer, Phys. Rev. Lett. **57**, 2649 (1986).

[20] J.N.M. Van Wunnik et al., Surf. Sci. **131**, 17 (1983).

[21] H. Winter, Comm. At. Mol. Phys. **26**, 287 (1991).

FIGURE CAPTIONS

Fig. 1 Projectile velocity dependence of the scattered neutral fractions for multicharged Cs, K, and Na projectiles (q=2-7) grazingly incident on LiF(100). The lines are fitted curves based on an analysis described in Ref. [12].

Fig. 2 Comparison of the angular distributions of scattered neutral and 1+ charge fractions for 5 keV Na^+ and Na^{2+} ions incident on LiF at small grazing angle; $v_\perp$= 2.0 and 2.7 x 10^{-3} a.u., respectively.

Fig. 3 Comparison of the angular distributions of scattered neutral and 1+ charge fractions for 4.5 keV Na^+ and Na^{3+} ions incident on LiF at larger grazing angle; $v_\perp$= 3.4 and 4.0 x 10^{-3} a.u., respectively.

Fig. 4 Perpendicular velocity dependence of the scattered neutral fraction for two different Cs multicharged ions incident on LiF at two fixed parallel velocities.

Fig. 5 Energy level diagram of single electron capture states for singly and doubly charged Na and Ne ions, juxtaposed with the valence bands of LiF, NaF, and Au.

Fig. 6 Projectile velocity dependence of the scattered neutral fractions for singly and multicharged Ne ions grazingly incident on LiF(100), together with the results of Hecht et al. for incident Ne^+ ions.

Fig. 7 Same as Fig. 3, but incident ions are Ne^+ and Ne^{3+}, at $v_\perp$= 1.5 and 2.3 x 10^{-3} a.u., respectively.

Fig. 8 Same as Fig. 7, but larger incident angle; $v_\perp$= 3.7 and 3.9 x 10^{-3} a.u., respectively.

Fig. 9 Same as Fig. 6, but for a NaF target.

Fig. 10 Highly schematic diagram of the possible neutralization pathway of a doubly charged incident Na ion that bypasses the blocked neutralization of the 1+ ion. Shown is double capture to the $3s^2 2p^5$ state, followed by Auger de-excitation (with the arrows labelled "1" and "2" indicating the two equivalent pair of transitions) which leaves the projectile in the $2p^6$ 3s ground state. For the purposes of this diagram, the indicated $3s^2$ level represents the average binding energy of the two equivalent electrons, and is thus not meant to accurately portray the individual binding energies of the two electrons.

Fig. 11 Projectile velocity dependence of the scattered neutral fraction for Na multicharged ions grazingly incident in Au(110).

Fig. 12 Projectile velocity dependence of the scattered negative fractions for O, F, and B singly and multiply charged ions grazingly incident on LiF(110). The lines are fitted curves based on an analysis described in Ref. [12].

Fig. 13 Same as Fig. 1 but for incident Ar singly and multiply charged ions.

Fig. 14 Target azimuthal orientation dependence of the scattered neutral fraction for 35 keV Cs^{7+} grazingly incident on LiF(100).

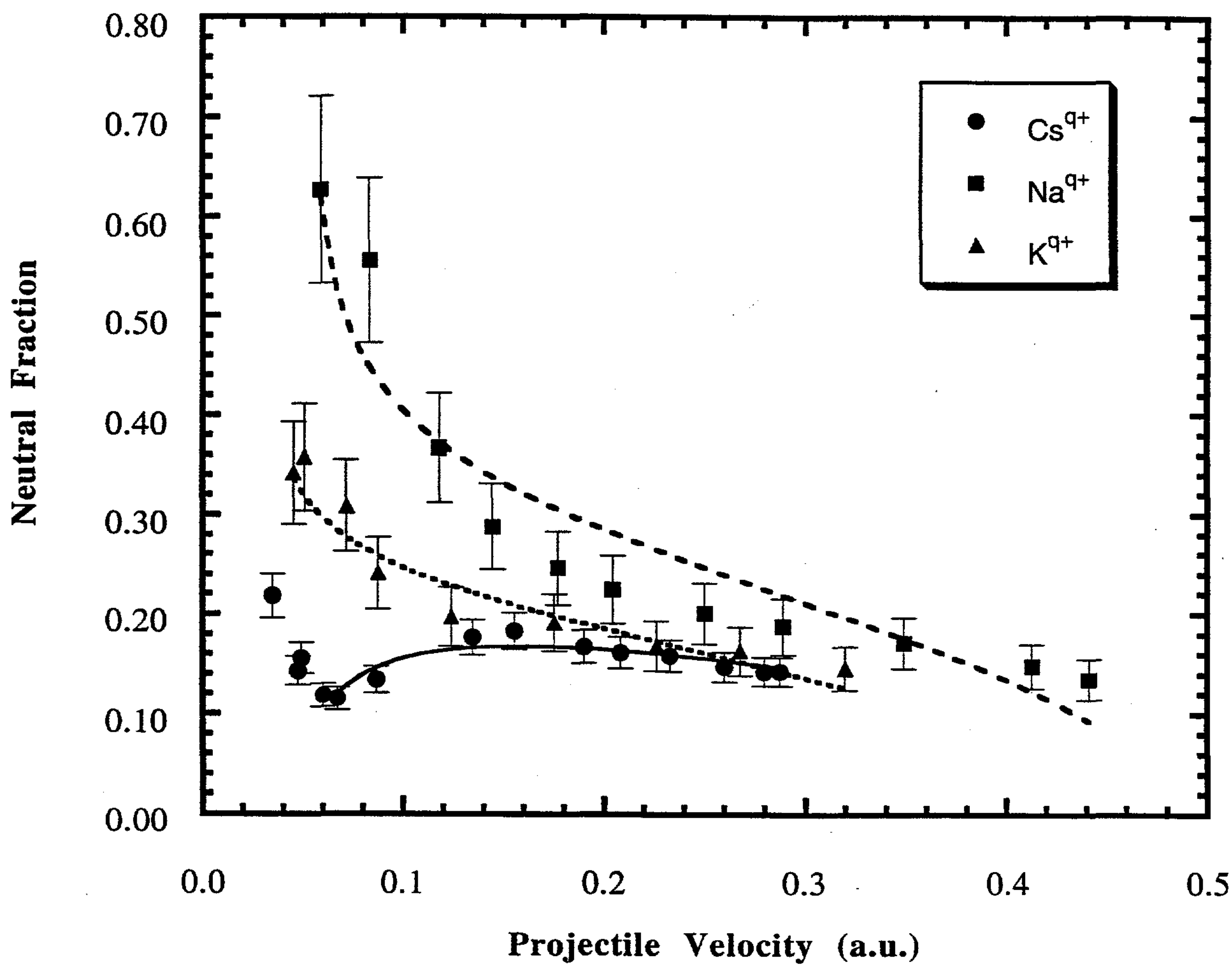

0.80
0.70
0.60
0.50
0.40
0.30
0.20
0.10
0.00
Neutral Fraction
0.0
0.1
0.2
0.3
0.4
0.5
Projectile Velocity (a.u.)
Cs^{q+}
Na^{q+}
K^{q+}

Fig. 1

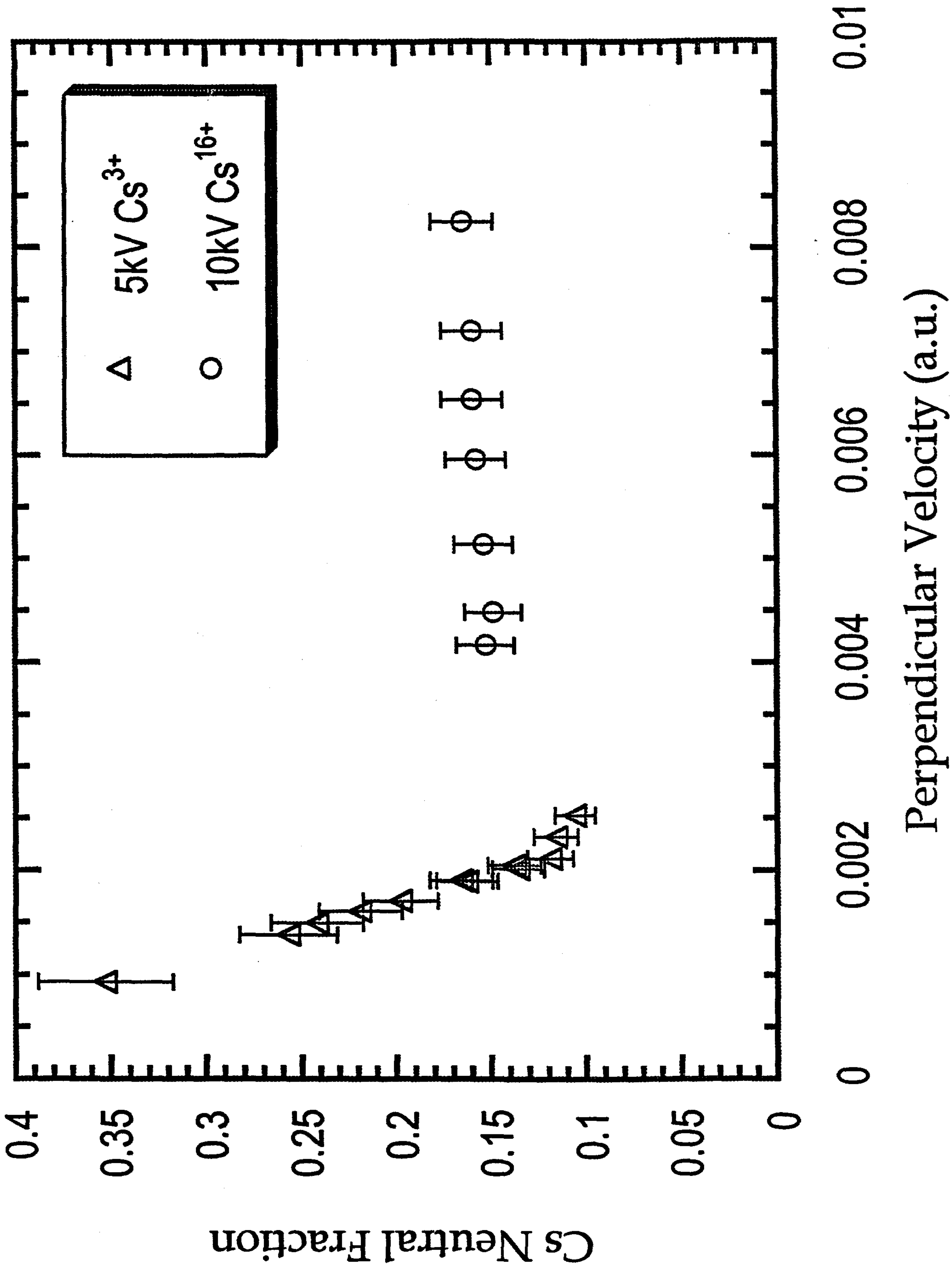

Cs Neutral Fraction
Perpendicular Velocity (a.u.)
5kV Cs3+
10kV Cs16+
0
0.05
0.1
0.15
0.2
0.25
0.3
0.35
0.4
0
0.002
0.004
0.006
0.008
0.01

Fig. 4

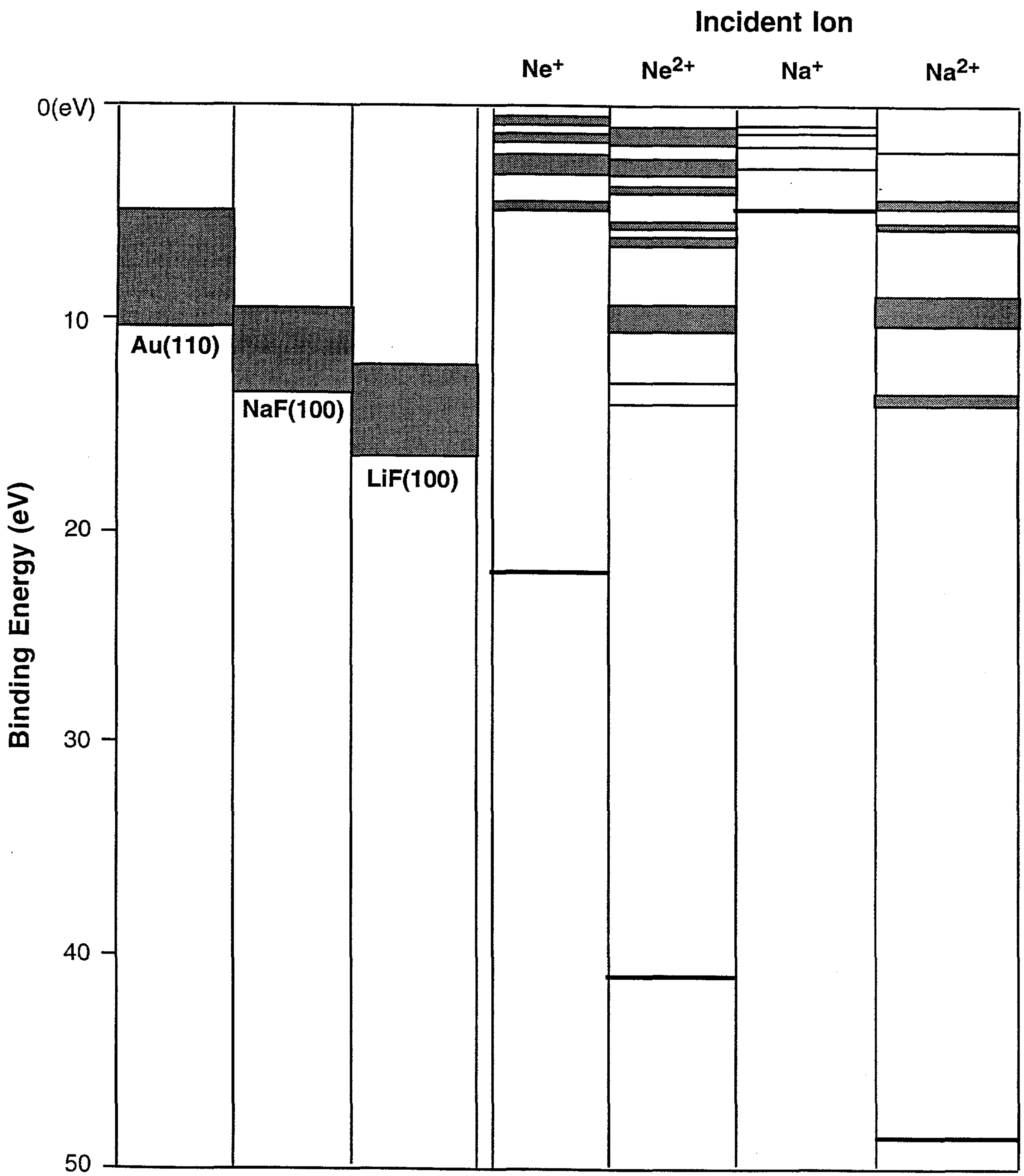
Incident Ion
Ne+
Ne2+
Na+
Na2+
0(eV)
10
20
30
40
50
Binding Energy (eV)
Au(110)
NaF(100)
LiF(100)

Fig. 5

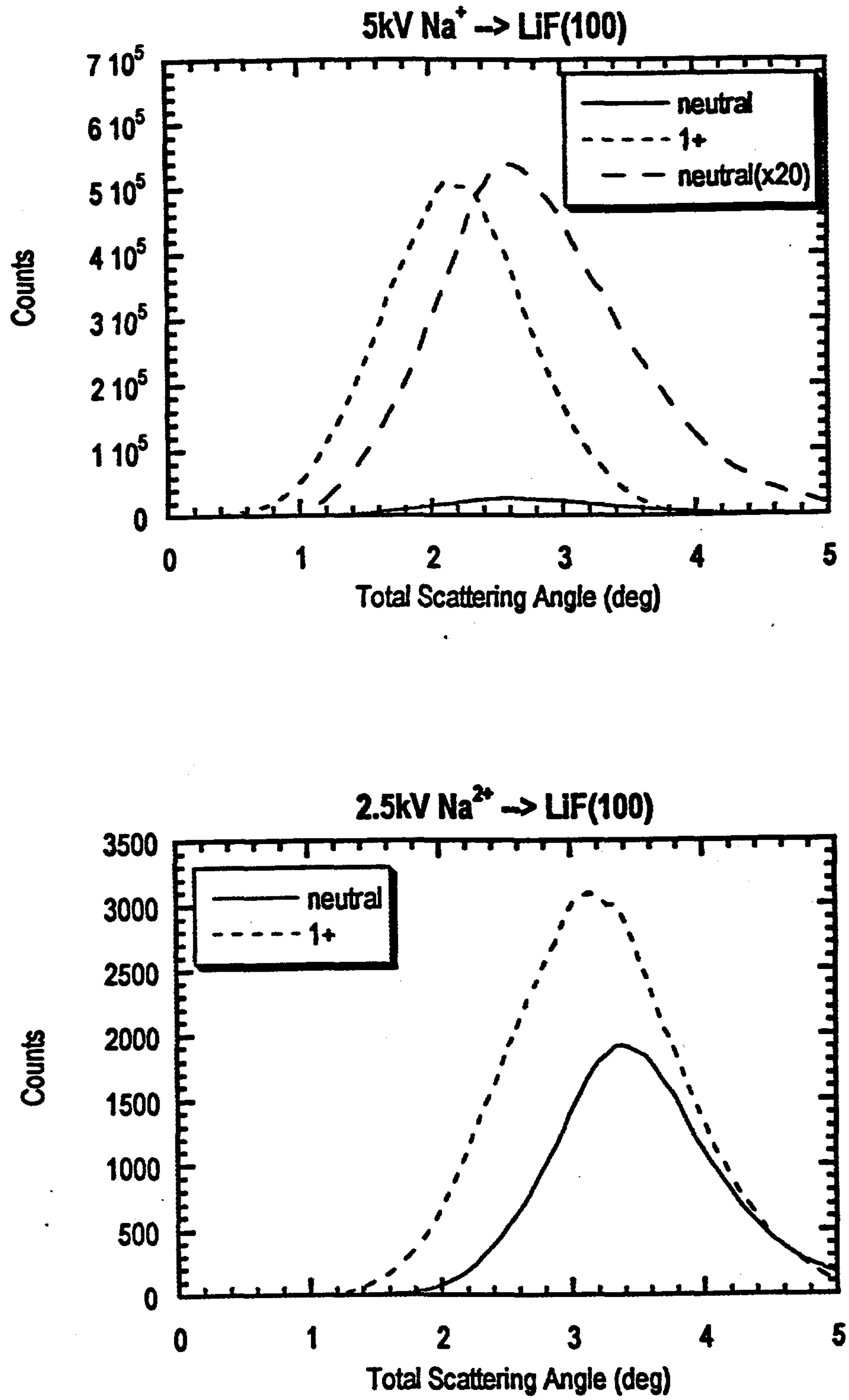
5kV Na+ --> LiF(100)
7 10^5
6 10^5
5 10^5
4 10^5
3 10^5
2 10^5
1 10^5
0
Counts
neutral
1+
neutral(x20)
0
1
2
3
4
5
Total Scattering Angle (deg)
2.5kV Na2+ --> LiF(100)
3500
3000
2500
2000
1500
1000
500
0
Counts
neutral
1+
0
1
2
3
4
5
Total Scattering Angle (deg)

Fig. 2

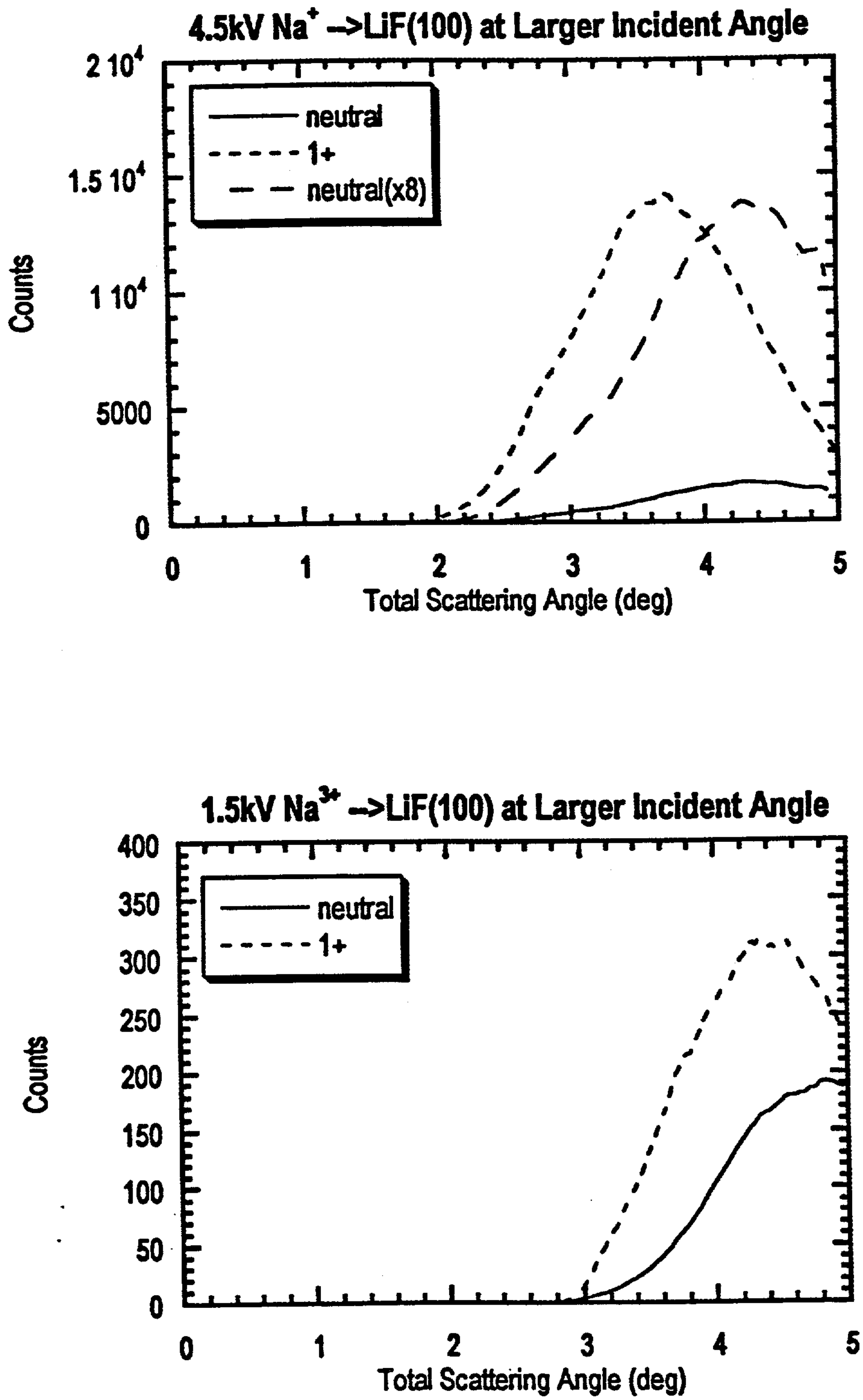
4.5kV Na+ ->LiF(100) at Larger Incident Angle
Counts
Total Scattering Angle (deg)
neutral
1+
neutral(x8)
2 10^4
1.5 10^4
1 10^4
5000
0
0
1
2
3
4
5
1.5kV Na3+ ->LiF(100) at Larger Incident Angle
Counts
Total Scattering Angle (deg)
neutral
1+
400
350
300
250
200
150
100
50
0
0
1
2
3
4
5

Fig. 3

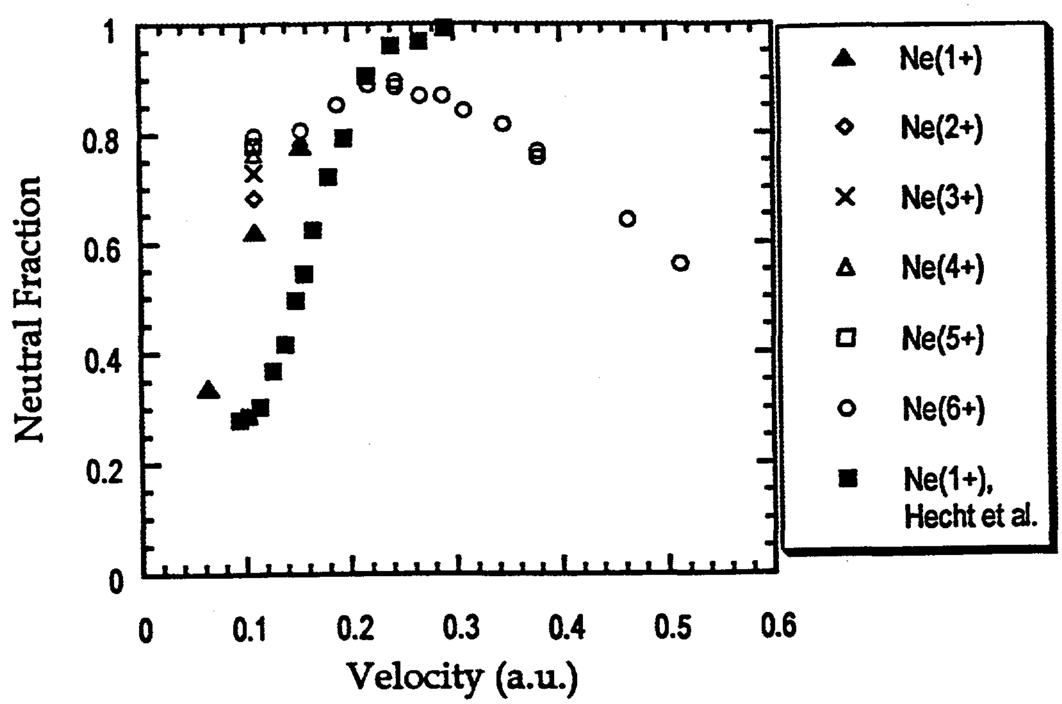

Neutral Fraction
1
0.8
0.6
0.4
0.2
0
0
0.1
0.2
0.3
0.4
0.5
0.6
Velocity (a.u.)
Ne(1+)
Ne(2+)
Ne(3+)
Ne(4+)
Ne(5+)
Ne(6+)
Ne(1+), Hecht et al.

Fig. 6

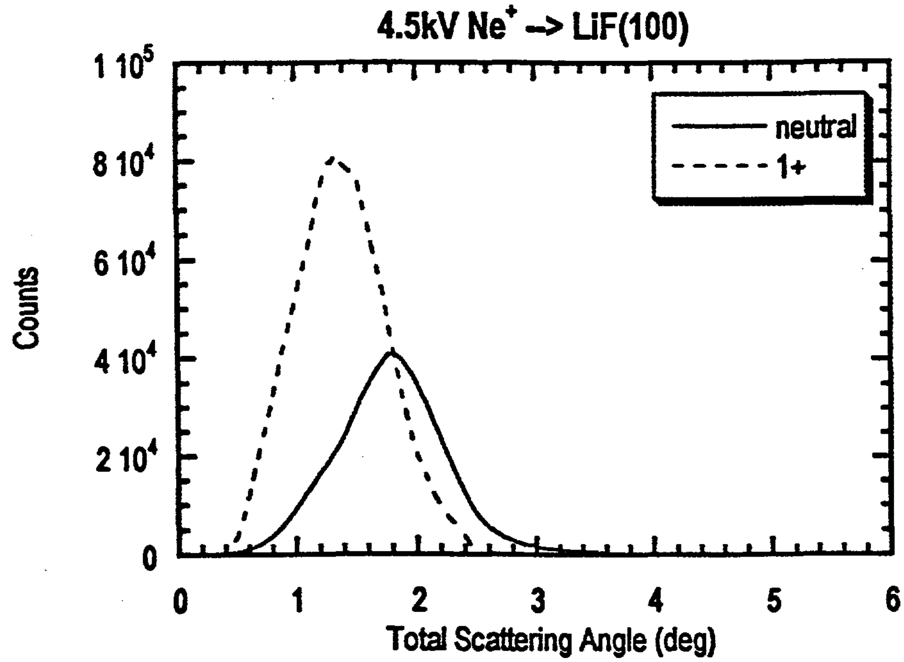
4.5kV Ne+ --> LiF(100)
Counts
Total Scattering Angle (deg)
neutral
1+
1 10^5
8 10^4
6 10^4
4 10^4
2 10^4
0
0
1
2
3
4
5
6

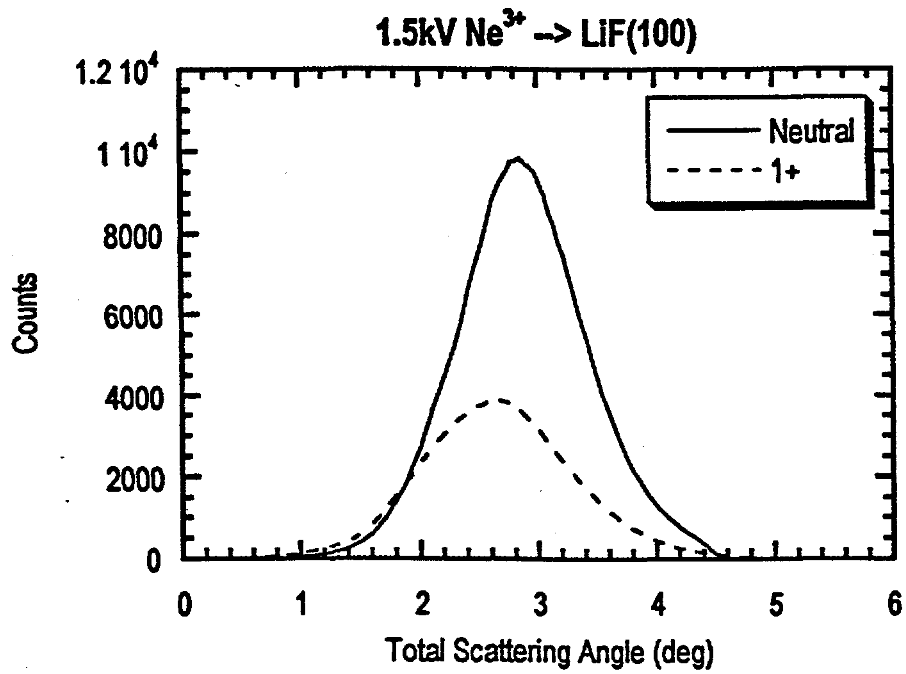
1.5kV Ne3+ --> LiF(100)
Counts
Total Scattering Angle (deg)
Neutral
1+
1.2 10^4
1 10^4
8000
6000
4000
2000
0
0
1
2
3
4
5
6

Fig. 7

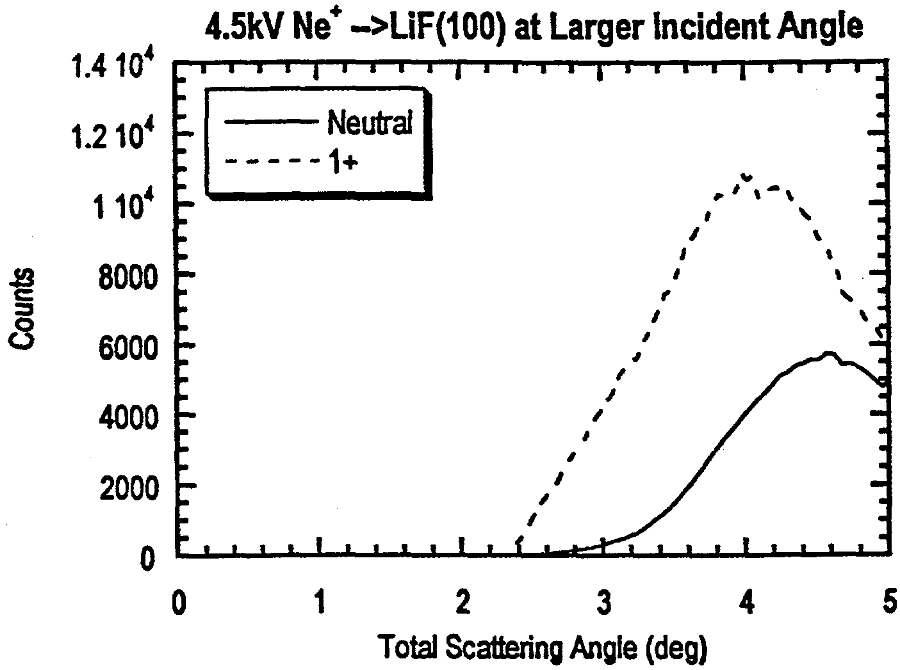
4.5kV Ne+ -->LiF(100) at Larger Incident Angle
1.4 10^4
1.2 10^4
1 10^4
8000
6000
4000
2000
0
Counts
Neutral
1+
0
1
2
3
4
5
Total Scattering Angle (deg)

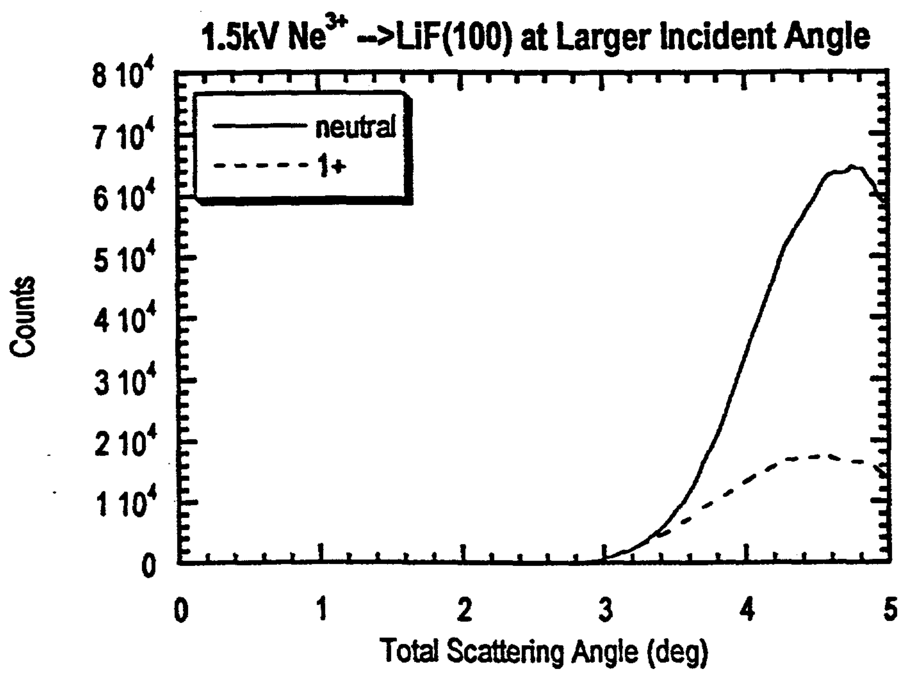
1.5kV Ne3+ -->LiF(100) at Larger Incident Angle
8 10^4
7 10^4
6 10^4
5 10^4
4 10^4
3 10^4
2 10^4
1 10^4
0
Counts
neutral
1+
0
1
2
3
4
5
Total Scattering Angle (deg)

Fig. 8

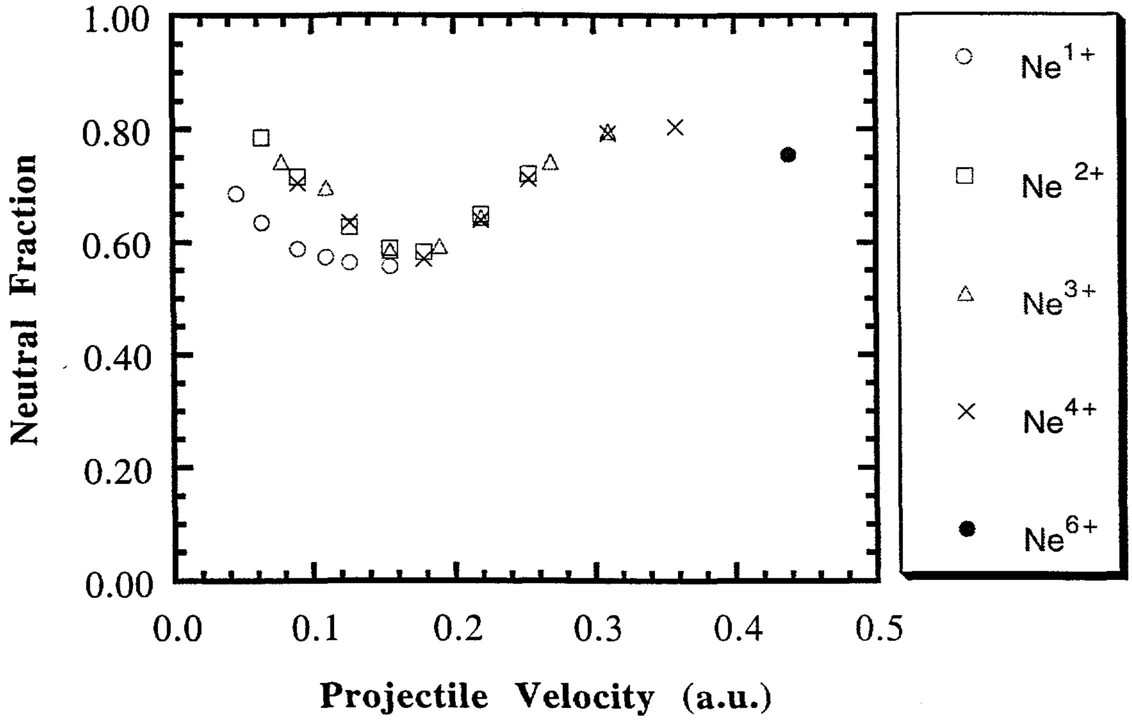
1.00
0.80
0.60
0.40
0.20
0.00
0.0
0.1
0.2
0.3
0.4
0.5
Neutral Fraction
Projectile Velocity (a.u.)
Ne1+
Ne 2+
Ne3+
Ne4+
Ne6+

Fig. 9

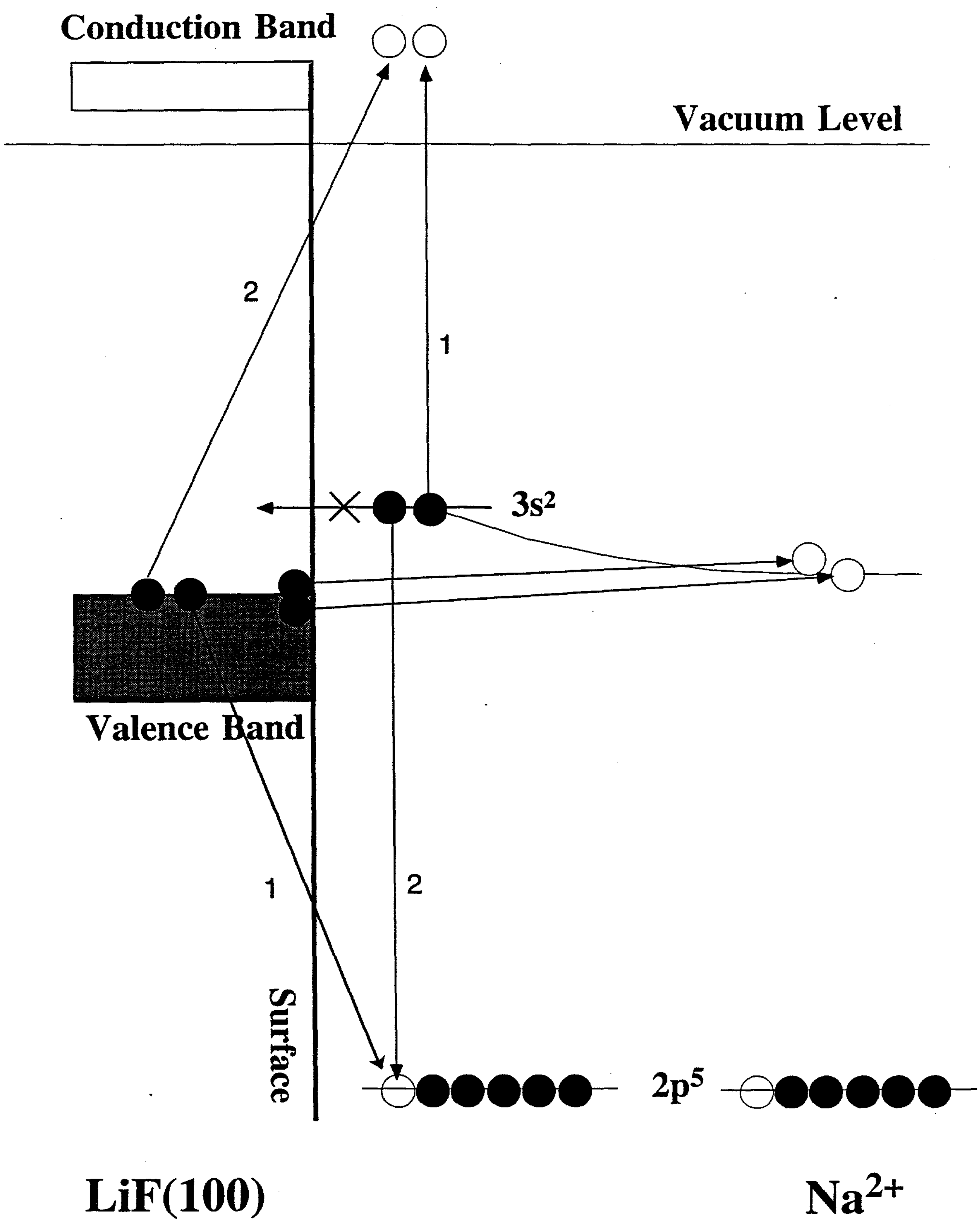

Conduction Band
Vacuum Level
2
1
3s²
Valence Band
1
2
Surface
2p⁵
LiF(100)
Na²⁺

Fig. 10

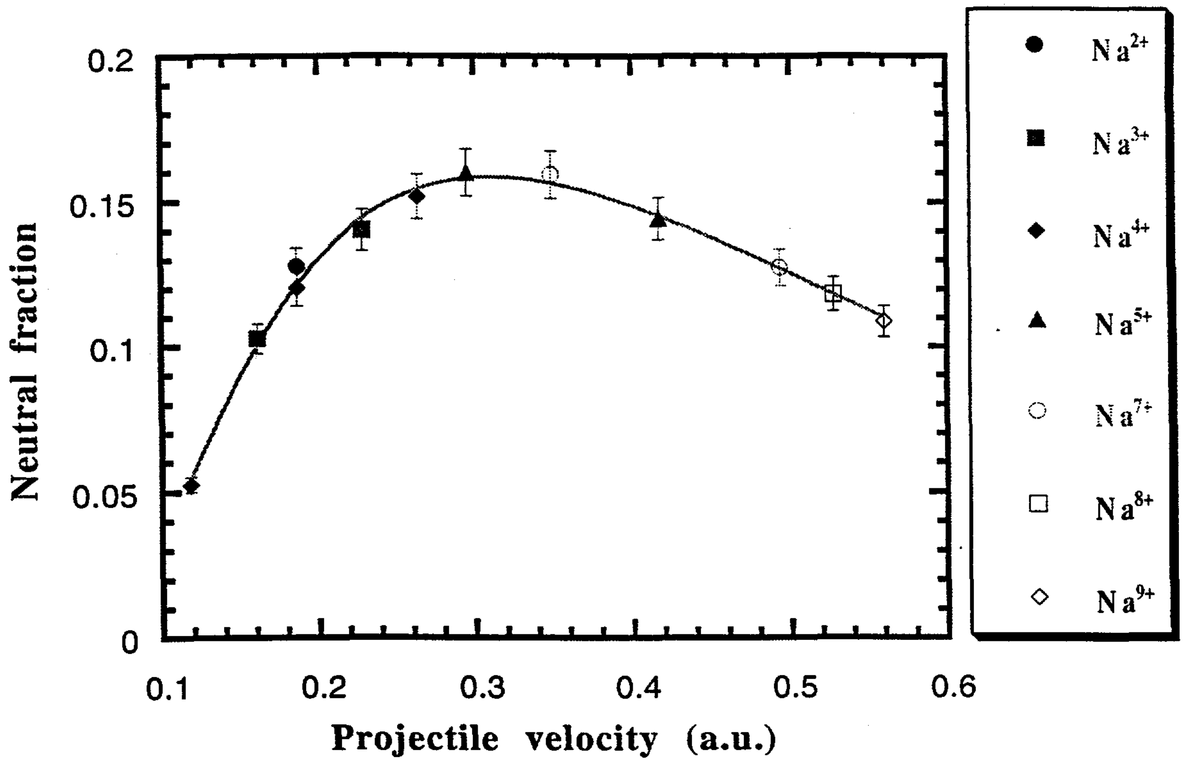

0.2
0.15
0.1
0.05
0
Neutral fraction
0.1
0.2
0.3
0.4
0.5
0.6
Projectile velocity (a.u.)
Na2+
Na3+
Na4+
Na5+
Na7+
Na8+
Na9+

Fig. 11

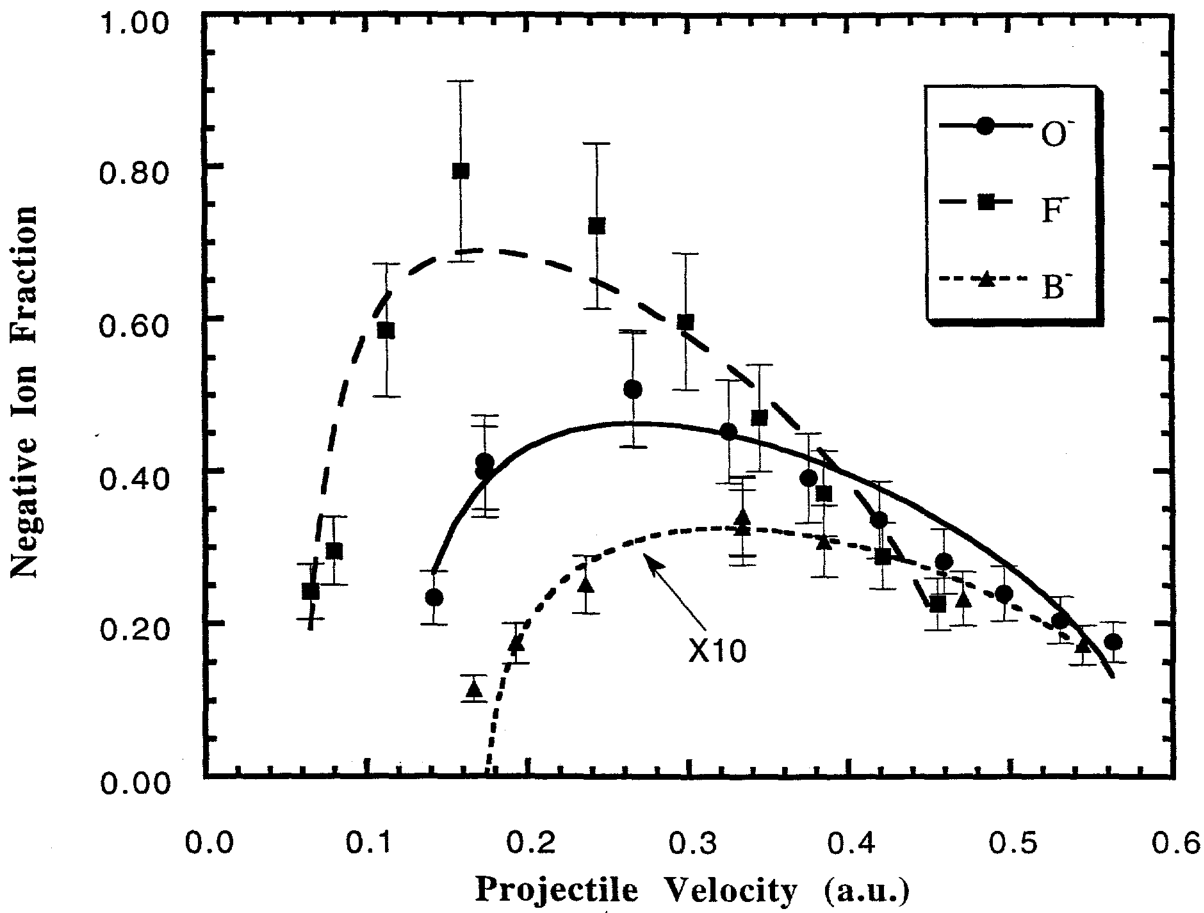

1.00
0.80
0.60
0.40
0.20
0.00
Negative Ion Fraction
0.0
0.1
0.2
0.3
0.4
0.5
0.6
Projectile Velocity (a.u.)
O⁻
F⁻
B⁻
X10

Fig. 12

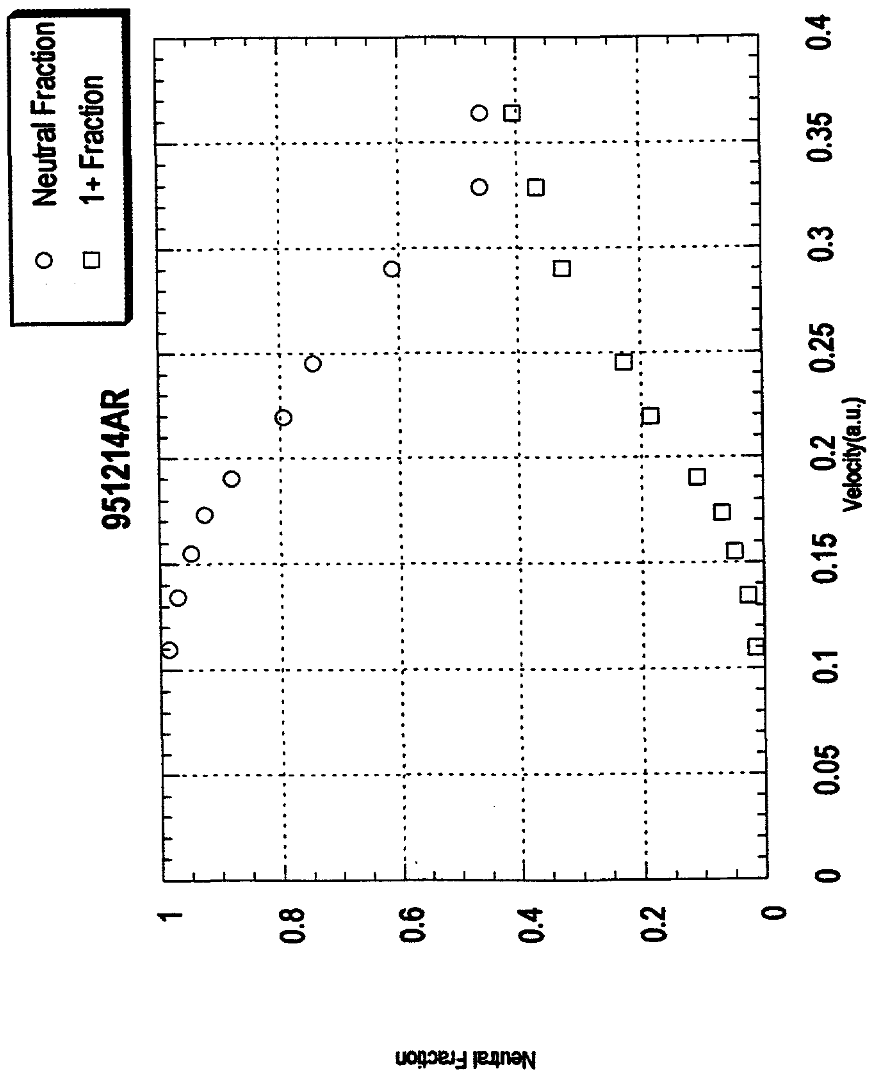
951214AR
Neutral Fraction
1+ Fraction
Velocity(a.u.)
Neutral Fraction
0
0.05
0.1
0.15
0.2
0.25
0.3
0.35
0.4
0.2
0.4
0.6
0.8
1

Fig. 13

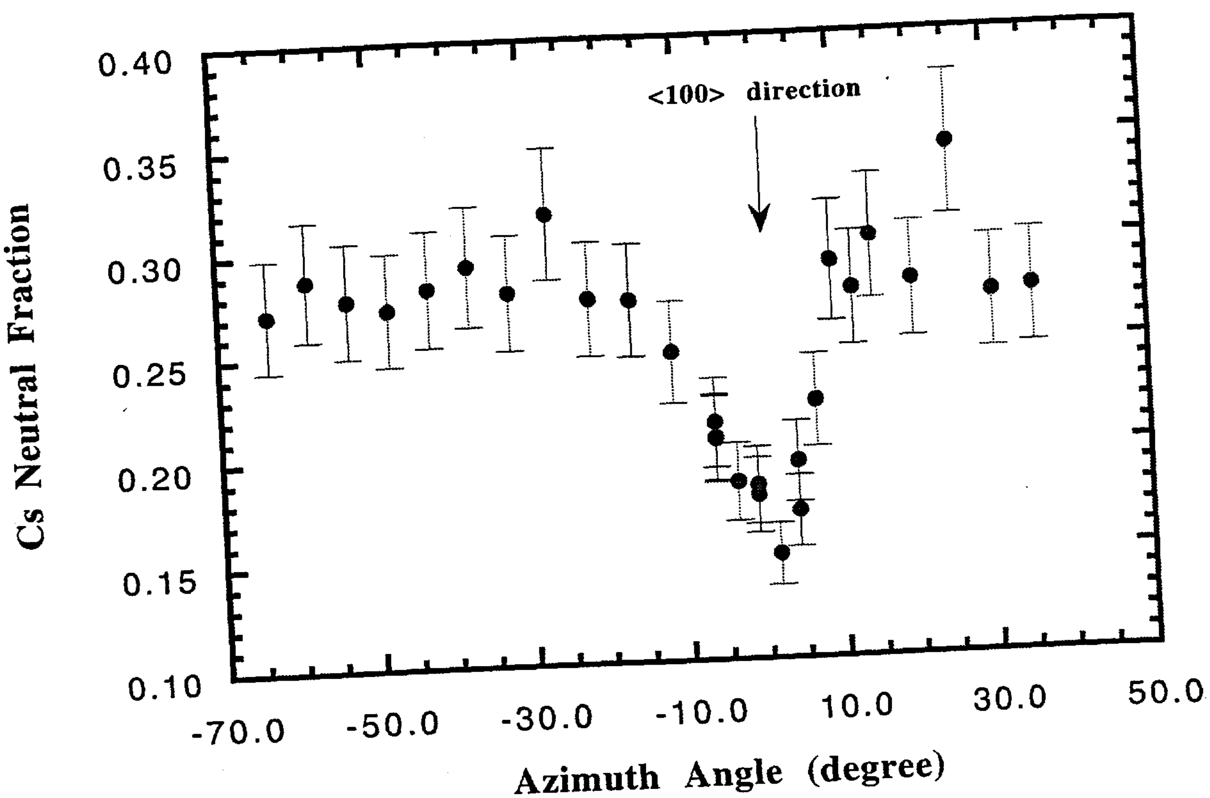

0.40
0.35
0.30
0.25
0.20
0.15
0.10
Cs Neutral Fraction
<100> direction
-70.0
-50.0
-30.0
-10.0
10.0
30.0
50.0
Azimuth Angle (degree)

Fig. 14